Traveling waves in phase-separating reactive mixtures

Tohru Okuzono* and Takao Ohta
Institute for Nonlinear Sciences and Applied Mathematics, Graduate School of Science, Hiroshima University, Higashi-Hiroshima 739-8526, Japan

(Received 24 May 2002; revised manuscript received 7 November 2002; published 21 May 2003)

A model of phase separation of chemically reactive ternary mixtures is constructed. In this model, spatially periodic structures that coherently propagate at a constant speed emerge through a Hopf bifurcation at a finite wave number. It is shown by computer simulations that both lamellar and hexagonal structures undergo a coherent propagating motion in two dimensions, and there are two types of traveling hexagons depending on the relative direction between the traveling velocity and the lattice vectors of the hexagonal structure. Amplitude equations for the traveling waves are derived, and the stability of the traveling and standing waves is discussed.

DOI: 10.1103/PhysRevE.67.056211 PACS number(s): 05.45.−a, 82.40.−g, 82.40.Ck

I. INTRODUCTION

Oscillation of spatially periodic structures appears in various systems far from equilibrium. One example is the oscillating roll structure in Rayleigh-Bénard convection of binary mixtures, where a dynamical coupling between the local concentration and the local temperature causes an overshoot of domain motion resulting in an oscillation (see Ref. [1] and the earlier references cited therein). Propagation of a stripe structure has also been observed experimentally in the electrohydrodynamic instability of liquid crystals [2]. These are macroscopic dynamic patterns out of equilibrium.

Other examples of formation of oscillating domains are microscopic. In contrast to the macroscopic nonequilibrium structures, it is emphasized here that phase transitions generally play a relevant role for the dynamics of microscopic domains. It has been found that adsorbates on metal surfaces exhibit propagating and/or standing oscillations of nano- or mesoscopic domains [3,4]. Hildebrand *et al.* [5] (see also [6]) introduced a model for traveling nanoscale stripe structures in surface chemical reactions and successfully reproduced the traveling stripe structure. In their model, nonlocal attractive interactions between adsorbates were considered, which cause a first order phase transition (phase separation) of the adsorbates. This property together with a chemical reaction between the adsorbates is the origin of the traveling waves.

It is worth mentioning that a traveling mesoscopic stripe pattern has also been observed experimentally in Langmuir monolayers [7]. Quite recently, this phenomenon has been studied theoretically by introducing a set of model equations that contains a phase separation mechanism [8].

In phase separation in thermal equilibrium, domains generally grow indefinitely. However, it is well known that the domain growth ceases at a certain length scale if chemical reactions take place [9–13]. The resulting domain structure is periodic in space but not necessarily oscillatory. The mechanism for formation of periodic structures is mathematically equivalent to the microphase separation in block copolymers [14,15].

The purpose of the present paper is to investigate, from a general point of view, self-propagation of microscopic cellular structures far from equilibrium. We consider a ternary mixture with components A, B, and C which undergo a chemical reaction $A \rightarrow B \rightarrow C \rightarrow A$. The reason for introducing this hypothetical cyclic linear reaction is that it is the simplest way to maintain the system far from equilibrium and hence most convenient to explore the features of nonequilibrium systems without being heavily involved in mathematical complications. The components A and B are assumed to be phase separated at low temperature. This is modeled by the usual Cahn-Hilliard type equation, which has been studied extensively for many years [16,17].

We make several comments on the cyclic reaction employed in the present paper. First of all, we mention that this reaction does not violate any thermodynamic law since we assume other chemical species D, E, ... which undergo chemical reactions such as $A+D \rightarrow B$. We do not consider them explicitly, assuming that they are supplied rapidly and have high mobility so that the concentrations are constant in space and time. Second, as a hypothetical experiment using the cyclic reaction, we consider an adsorbed system on a substrate supplied from the gas phase. Suppose that the substrate has a square lattice divided by two sublattices like a checkerboard, and that the irrelevant species like D occupy only one of the sublattices (black sublattice) whereas the molecules A and B occupy only the other sublattice (white sublattice). We assign the component C as empty sites of the white sublattice. The reaction $A+D \rightarrow B$ is assumed to take place as a bimolecular conversion, the reaction $B \rightarrow C$ is a desorption of the species B to the gas phase, and the reaction $C \rightarrow A$ is interpreted as the adsorption of molecules A from the gas phase. In this way, a cyclic reaction is achieved, which is irreversible as a whole because of the consumption of D.

The present study is a fusion of the theory of phase transitions and physics of nonequilibrium systems. So far these two subjects have been thought of as unrelated problems. Recently, however, a combined study of these different fields

*Present address: Yokoyama Nano-structured Liquid Crystal Project, ERATO, Japan Science and Technology Corporation, 5-9-9 Tokodai, Tsukuba 300-2635, Japan.

has been anticipated, for instance, to control various nanoscale structures.

Our main concern is the self-organized propagation not only of stripe structures but also of hexagonal structures in two dimensions. We will show in computer simulations of the present system that both a lamellar structure and a hexagonal structure exhibit coherent self-propulsion when the uniform stationary state becomes unstable.

A traveling hexagonal pattern has been obtained in the damped Kuramoto-Sivashinsky equation [18] and in a model equation for a neural field [19]. In these systems, the traveling structures appear as a secondary bifurcation after forming a motionless structure. Compared with these studies, we believe that our system of ternary reactive mixtures has a wider applicability, showing that both lamellae and hexagons can travel in a self-organized manner. The preliminary results have been published in Ref. [20].

The organization of this paper is as follows. In the next section, we construct a model for phase-separating ternary reactive mixtures and perform a linear stability analysis of the model equations. In Sec. III we carry out numerical simulations of our model in one and two dimensions. It is shown that both lamellar and hexagonal structures in two dimensions can travel through a Hopf bifurcation at a finite wave number. In Sec. IV we derive the amplitude equations for a supercritical Hopf bifurcation from our model equations. The stabilities of traveling and standing wave solutions of the amplitude equations are analyzed, and the phase dynamics of the traveling lamellar structure in one and two dimensions is also developed. In Sec. V we discuss theoretically the traveling hexagonal structures, considering the amplitude equations obtained by the single mode approximation. Finally, we summarize our work and touch on future problems in Sec. VI.

II. CHEMICALLY REACTIVE TERNARY MIXTURES

A. Generic model

Let us consider a ternary reactive mixture that consists of molecules of type *A*, *B*, and *C* and denote their local concentrations by ψ_A, ψ_B, and ψ_C, respectively. When the normalization condition $\psi_A+\psi_B+\psi_C=1$ is satisfied at each space point, two of these variables are chosen to be independent. Hence we define the local kinetic variables $\psi(\mathbf{r},t)$ and $\phi(\mathbf{r},t)$ at position $\mathbf{r}$ and time t as $\psi=\psi_A-\psi_B$ and $\phi=\psi_A+\psi_B$. We assume that these variables obey the following type of kinetic equation:

$$\frac{\partial\psi}{\partial t}=\nabla\cdot\left(M_1\nabla\frac{\delta F}{\delta\psi}\right)+f(\psi,\phi), \tag{1}$$

$$\frac{\partial\phi}{\partial t}=\nabla\cdot\left(M_2\nabla\frac{\delta F}{\delta\phi}\right)+g(\psi,\phi), \tag{2}$$

where M_1 and M_2 are the mobilities associated with ψ and ϕ and are assumed to be positive constants, although they may depend on ψ and ϕ in general. F is a free energy functional of Ginzburg-Landau type:

$$F=\int d\mathbf{r}\left[\frac{D_1}{2}|\nabla\psi|^2+\frac{D_2}{2}|\nabla\phi|^2+w(\psi,\phi)\right], \tag{3}$$

where D_1 and D_2 are positive constants and $w(\psi,\phi)$ is a potential function. The last terms of Eqs. (1) and (2) are reaction terms, and $f(\psi,\phi)$ and $g(\psi,\phi)$ are, in general, nonlinear functions of ψ and ϕ.

The kinetics of block-copolymer systems is described by the same type of equations as Eqs. (1) and (2). In this case, $f(\psi,\phi)$ and $g(\psi,\phi)$, which are linear in ψ and ϕ, come from the nonlocal interaction between monomers.

Here we study the linear stability of the uniform equilibrium solution $\psi=\psi_0$ and $\phi=\phi_0$, determined by $f(\psi_0,\phi_0)=0$ and $g(\psi_0,\phi_0)=0$. Using the Fourier components ψ_q and ϕ_q with wave number q for the deviation of ψ and ϕ from ψ_0 and ϕ_0, respectively, we have the linearized forms of Eqs. (1) and (2) as

$$\frac{d}{dt}\begin{pmatrix}\psi_q\\ \phi_q\end{pmatrix}=\mathcal{L}_q\begin{pmatrix}\psi_q\\ \phi_q\end{pmatrix}, \tag{4}$$

where the linear evolution matrix $\mathcal{L}_q$ is given by

$$\mathcal{L}_q=-q^2\mathcal{M}(q^2\mathcal{D}+\mathcal{W})+\mathcal{A}, \tag{5}$$

where $\mathcal{M}$ and $\mathcal{D}$ are diagonal matrices defined as $\mathcal{M}=\mathrm{diag}(M_1,M_2)$ and $\mathcal{D}=\mathrm{diag}(D_1,D_2)$, and $\mathcal{W}=(w_{ij})$ and $\mathcal{A}=(a_{ij})$ $(i,j=1,2)$ are matrices with components $w_{11}=w_{\psi\psi}(\psi_0,\phi_0)$, $w_{12}=w_{21}=w_{\psi\phi}(\psi_0,\phi_0)$, $w_{22}=w_{\phi\phi}(\psi_0,\phi_0)$, $a_{11}=f_\psi(\psi_0,\phi_0)$, $a_{12}=f_\phi(\psi_0,\phi_0)$, $a_{21}=g_\psi(\psi_0,\phi_0)$, and $a_{22}=g_\phi(\psi_0,\phi_0)$, where the functions with the subscripts ψ and ϕ mean the partial derivatives with respect to their variables. Note that the matrix $\mathcal{W}$ is always symmetric, whereas the matrix $\mathcal{A}$ is, in general, not symmetric, although it is symmetric for block-copolymer systems.

The eigenvalues λ_q of $\mathcal{L}_q$ determine the linear stability of the uniform equilibrium solution. One of the control parameters for the stability in our model is the temperature T, which enters through w_{11} and w_{22} which are linear functions of T. Hereafter, we introduce for convenience the control parameter τ instead of T, such that the uniform state becomes unstable as τ increases. Note that $\mathcal{W}$ determines the thermodynamic stability of the uniform state (ψ_0,ϕ_0), which is stable if $w_{11}\geqslant 0$ and $\det\mathcal{W}\geqslant 0$ in the absence of chemical reactions.

Since the eigenvalues of $-q^2\mathcal{M}(q^2\mathcal{D}+\mathcal{W})$ are always real, the properties of $\mathcal{A}$ prescribe the type of instability. For simplicity, we set $M_1=M_2=1$ below, which does not change the essence of the following argument. Suppose the system of ordinary differential equations for Eqs. (1) and (2) ($q=0$ mode) is stable, that is,

$$\mathrm{tr}\,\mathcal{A}<0 \quad \text{and} \quad \det\mathcal{A}>0. \tag{6}$$

As τ is increased, the largest $\mathrm{Re}\,\lambda_q$ becomes positive at a finite wave number $q=q_c\neq 0$ and either Turing-type $(\mathrm{Im}\,\lambda_{q_c}=0)$ or Hopf-type $(\mathrm{Im}\,\lambda_{q_c}\neq 0)$ instabilities occur depending on $\mathcal{A}$. When $\det\mathcal{L}_{q_c}=0$ and $\mathrm{tr}\,\mathcal{L}_{q_c}<0$, the Turing-type instability occurs. In this case we expect that

stationary (motionless) periodic structures emerge. On the other hand, the Hopf-type instability, which we are concerned with, occurs when $\det \mathcal{L}_{q_c} > 0$ and

$$\mathrm{tr}\, \mathcal{L}_{q_c} = \frac{(\mathrm{tr}\, \mathcal{W})^2}{4\, \mathrm{tr}\, \mathcal{D}} + \mathrm{tr}\, \mathcal{A} = 0 \tag{7}$$

with

$$q_c^2 = -\frac{\mathrm{tr}\, \mathcal{W}}{2\, \mathrm{tr}\, \mathcal{D}} \tag{8}$$

for $\mathrm{tr}\, \mathcal{W} < 0$. In this case a traveling wave or a standing oscillation is expected to be revealed.

The above analysis implies that an oscillatory instability at a finite wave number, which is sometimes called a wave instability, is induced by the thermodynamic instability of phase separation. A wave instability also occurs in the FitzHugh-Nagumo model with nonlocal coupling where drifting domains have been observed [21]. It should be noted that in block-copolymer systems only Turing-type instabilities can occur since the system is variational.

B. Simplified model and its linear stability

Now we construct a concrete model which shows self-propagation of spatially periodic structures. We start with the lattice gas Hamiltonian for a ternary mixture:

$$H = -\frac{1}{2} \sum_{\mathbf{i}, \boldsymbol{\delta}} \sum_{\alpha, \beta} J_{\alpha\beta} \hat{\psi}_\alpha(\mathbf{i}) \hat{\psi}_\beta(\mathbf{i} + \boldsymbol{\delta}), \tag{9}$$

where $\mathbf{i}$ denotes the lattice point and $\boldsymbol{\delta}$ stands for the nearest neighbor vector ($|\boldsymbol{\delta}| = 1$). $\hat{\psi}_\alpha(\mathbf{i}) = 1$ when the lattice point $\mathbf{i}$ is occupied by an α molecule, and otherwise equals zero. The coefficient $J_{\alpha\beta}$ is the interaction constant between α and β molecules, and $\alpha, \beta = A, B, C$. We are assuming that the interaction between A and B molecules is repulsive, i.e., $J_{AB} < 0$, and that C molecules are neutral for both A and B molecules. For simplicity, we hereafter consider the symmetric case, that is, $\chi_{AC} = \chi_{BC}$, where $\chi_{AC} \equiv -J_{AC} + (J_{AA} + J_{CC})/2$ and $\chi_{BC} \equiv -J_{BC} + (J_{BB} + J_{CC})/2$. By using the mean field approximation and taking the continuum limit, one can readily obtain the free energy functional in the form of Eq. (3). Since this procedure is standard [22], we do not describe it in detail. The coefficients D_1 and D_2 are given, respectively, by

$$D_1 = \frac{J_{AA} + J_{BB}}{4} - \frac{J_{AB}}{2}, \tag{10}$$

$$D_2 = \frac{J_{AA} + J_{BB}}{4} + \frac{J_{AB}}{2} + J_{CC} - J_{AC} - J_{BC}. \tag{11}$$

The uniform part w in Eq. (3) is given by the expansion as

$$w = -\frac{\tau}{2} \psi^2 + \frac{u}{4} \psi^4 + \frac{K}{2} (\phi - \phi_c)^2, \tag{12}$$

where

$$\tau \equiv 2D_1 - \frac{1}{\phi_c}, \tag{13}$$

$$u \equiv \frac{1}{3\phi_c^3}, \tag{14}$$

$$K \equiv \frac{2D_1}{1 - 2\phi_c} + \frac{1}{\phi_c(1 - \phi_c)} + \frac{2}{1 - 2\phi_c} \ln \frac{\phi_c}{2(1 - \phi_c)}, \tag{15}$$

and the higher order couplings between ψ and ϕ are omitted in Eq. (12). The constant ϕ_c is the spatial average of ϕ ($0 < \phi_c < 1$).

As is well known in the theory of phase separation [22], the D_1 term cannot be ignored in stabilizing the short wavelength modes in the phase-separated state. On the other hand, the D_2 term does not cause this difficulty so that we omit this term for simplicity. The last term in Eq. (12) produces a diffusion term $M_2 K \nabla^2 \phi$ in the kinetic equation (2). We will ignore this term by putting $K = 0$ in most of this paper. The effect of this diffusion does not essentially change the domain dynamics, as will be shown in Sec. VI. By comparing Eqs. (13) and (15), it is evident that the absence of diffusion of ϕ does not impose any restriction of the diffusion of ψ.

Based on the above considerations, we can greatly simplify the model equations (1) and (2). Under the further assumption $M_1 = M_2$, Eqs. (1) and (2) become, with appropriately scaled variables (we use the same symbols for the rescaled variables),

$$\frac{\partial \psi}{\partial t} = \nabla^2 [-D_1 \nabla^2 \psi - \tau \psi + \psi^3] + f(\psi, \phi), \tag{16}$$

$$\frac{\partial \phi}{\partial t} = g(\psi, \phi). \tag{17}$$

A Landau-type expansion of the potential (12) is valid for the weak segregation regime near the phase-separation temperature $\tau = 0$. We have verified in the numerical simulations shown in Sec. III that the spatial variations of ψ and ϕ do not deviate substantially from a sinusoidal function. Thus the present treatment has internal consistency.

Suppose that the system undergoes the following cyclic chemical reactions:

$$A \xrightarrow{\gamma_1} B \xrightarrow{\gamma_2} C \xrightarrow{\gamma_3} A, \tag{18}$$

where γ_1, γ_2, and γ_3 are the reaction rates. From the mass action law, the reaction terms in Eqs. (16) and (17) can be written as

$$f(\psi, \phi) = -\left(\gamma_1 + \frac{\gamma_2}{2} \right) \psi - \left(\gamma_1 - \frac{\gamma_2}{2} + \gamma_3 \right) \phi + \gamma_3, \tag{19}$$

$$g(\psi, \phi) = \frac{\gamma_2}{2} \psi - \left(\frac{\gamma_2}{2} + \gamma_3 \right) \phi + \gamma_3. \tag{20}$$

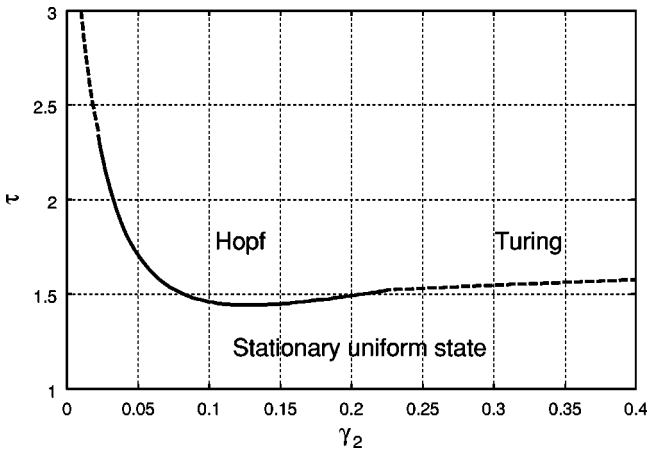

FIG. 1. Linear stability diagram for Eqs. (16) and (17) with Eqs. (19) and (20) in τ-γ_2 plane for $D_1=1$, $\gamma_1=0.3$, and $\gamma_3=0.05$. The solid and dashed lines in this figure indicate the Hopf- and Turing-type instabilities, respectively. All the quantities in this figure and Figs. 2–8 below are dimensionless.

In this case, the stationary uniform solutions ψ_0 and ϕ_0 are given by

$$\psi_0=\frac{\gamma_3(\gamma_2-\gamma_1)}{\gamma_1\gamma_2+\gamma_2\gamma_3+\gamma_3\gamma_1}, \tag{21}$$

$$\phi_0=\frac{\gamma_3(\gamma_2+\gamma_1)}{\gamma_1\gamma_2+\gamma_2\gamma_3+\gamma_3\gamma_1}, \tag{22}$$

and the matrix $\mathcal{A}$ is given by

$$\mathcal{A}=\begin{pmatrix} -\left(\gamma_1+\frac{\gamma_2}{2}\right) & -\left(\gamma_1-\frac{\gamma_2}{2}+\gamma_3\right) \\ \frac{\gamma_2}{2} & -\left(\frac{\gamma_2}{2}+\gamma_3\right) \end{pmatrix}. \tag{23}$$

A Hopf-type instability occurs when

$$\gamma_1\gamma_2+\gamma_2\gamma_3+\gamma_3\gamma_1-\left(\frac{\gamma_2}{2}+\gamma_3\right)(\gamma_1+\gamma_2+\gamma_3)>0 \tag{24}$$

and

$$\frac{(\tau-3\psi_0^2)^2}{4D_1}-(\gamma_1+\gamma_2+\gamma_3)=0 \tag{25}$$

at $q=q_c$ where

$$q_c=\left(\frac{\tau-3\psi_0^2}{2D_1}\right)^{1/2}. \tag{26}$$

The critical value τ_c is given from Eq. (25) by

$$\tau_c=3\psi_0^2+2\sqrt{D_1(\gamma_1+\gamma_2+\gamma_3)}. \tag{27}$$

The other solution of Eq. (25) is unphysical since it causes $q_c^2<0$.

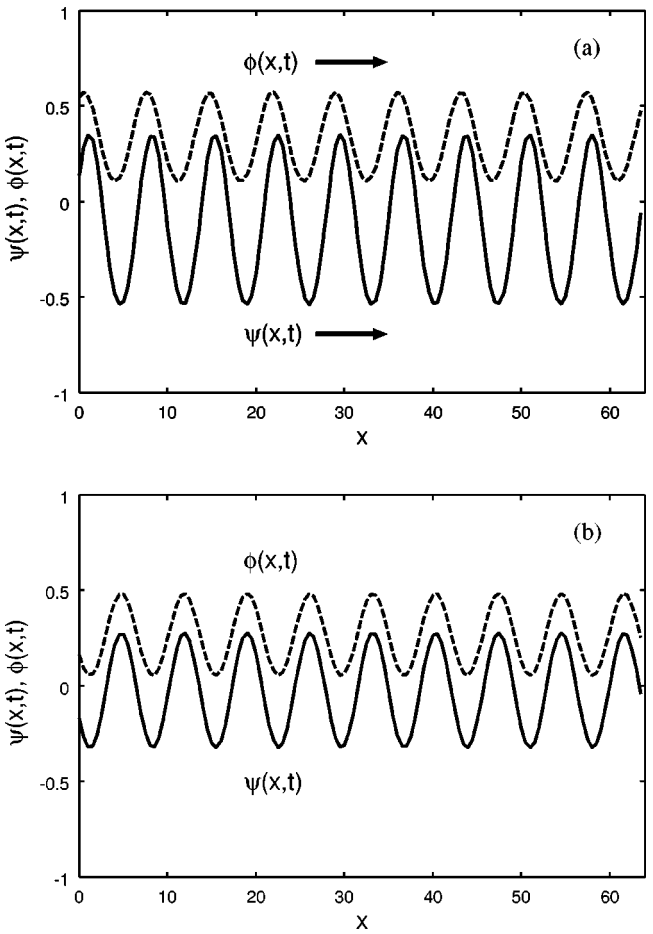

FIG. 2. Spatial profiles of $\psi(x,t)$ (solid lines) and $\phi(x,t)$ (dashed lines) obtained by one-dimensional simulations for (a) $\tau=1.6$, $\gamma_2=0.15$ (just above the Hopf instability line) and (b) $\tau=1.6$, $\gamma_2=0.25$ (just above the Turing instability line) at $t=5000$. Both profiles of $\psi(x,t)$ and $\phi(x,t)$ are propagating in the x direction indicated by the arrow with the same velocity in the case of (a), whereas they are stationary in the case of (b).

The linear stability diagram for Eqs. (16) and (17) with Eqs. (19) and (20) in the τ-γ_2 plane is shown in Fig. 1 for $D_1=1$, $\gamma_1=0.3$, and $\gamma_3=0.05$. The solid and dashed lines in this figure indicate the Hopf- and Turing-type instabilities, respectively. The stationary uniform state is stable for parameters below these lines.

III. NUMERICAL SIMULATIONS

In this section, we shall show, in one and two dimensions, the results obtained by computer simulations of Eqs. (16) and (17) with Eqs. (19) and (20) above the stability lines in Fig. 1.

First, we confirm numerically that a propagating solution exists in one dimension. The space mesh and the time increment have been set as 0.5 and 0.001, respectively. Figure 2(a) shows such a solution for $\tau=1.6$ and $\gamma_2=0.15$, which is just above the Hopf instability line (the solid line in Fig. 1). In Fig. 2(a) the profiles of $\psi(x,t)$ (solid line) and $\phi(x,t)$ (dashed line) are plotted as functions of the spatial coordi-

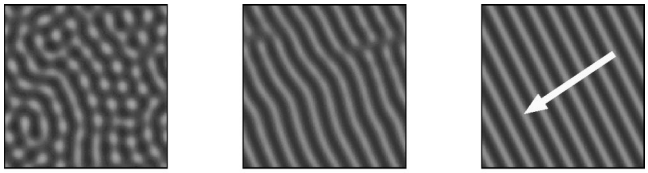

FIG. 3. Snapshots of $\psi(\mathbf{r},t)$, indicated in gray scale increasing from black to white, at $t=50$ (a), 500 (b), and 5000 (c) for $\tau=1.6$ and $\gamma_2=0.2$. The white arrow indicates the direction of propagation of the lamellar structure.

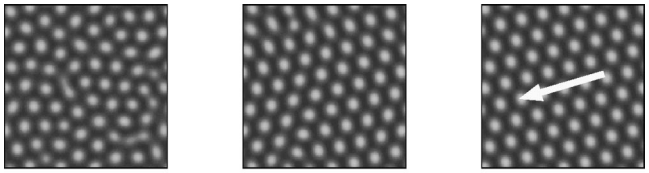

FIG. 4. Snapshots of $\psi(\mathbf{r},t)$ indicated in gray scale increasing from black to white at $t=50$ (a), 500 (b), and 5000 (c) for $\tau=1.6$ and $\gamma_2=0.1$. The white arrow indicates the direction of propagation of the hexagonal structure (type I).

nate x at $t=5000$. Both profiles of $\psi(x,t)$ and $\phi(x,t)$ are moving to the right, in this case, at a constant speed keeping their shapes and the phase difference between them, whereas Fig. 2(b) depicts stationary patterns of ψ and ϕ without a phase difference for $\tau=1.6$ and $\gamma_2=0.25$ above the Turing instability line.

A. Traveling lamellar pattern

Now we extend the simulations to two dimensions. The simulations have been carried out on a 128×128 square lattice with the mesh size $\Delta x=0.5$ using the finite difference Euler scheme with a fixed time step $\Delta t=10^{-3}$ for several values of parameters τ and γ_2. Other parameters are fixed at $D_1=1$, $\gamma_1=0.3$, and $\gamma_3=0.05$. As the initial conditions we start with homogeneous states with small random perturbations which satisfy $\langle\psi\rangle=\psi_0$ and $\langle\phi\rangle=\phi_0$ and use periodic boundary conditions, where the angular brackets mean spatial averages.

As predicted by the linear stability analysis, no pattern appears for parameters below the solid or dashed lines in Fig. 1. For parameters above the dashed line at which the Turing-type instability occurs, stationary lamellar or hexagonal patterns appear, depending on the equilibrium values of ψ_0 and ϕ_0. For parameters above the Hopf-type instability line (solid line in Fig. 1), various traveling patterns are observed. Henceforth, we concentrate on the parameter region near the Hopf instability line.

Figure 3 displays three snapshots of $\psi(\mathbf{r},t)$, indicated in gray scale increasing from black to white, at $t=50$ (a), 500 (b), and 5000 (c) for $\tau=1.6$ and $\gamma_2=0.2$ ($\psi_0=-0.059$, $\phi_0=0.29$). In the early stage, irregular patterns with motions of distorted standing waves are formed [Fig. 3(a)]. After this transient regime, partially coherent lamellar structures which are traveling emerge [Fig. 3(b)]. The system eventually reaches a state in which the lamellar structure extended to the whole system is traveling at a constant speed [Fig. 3(c)]. The arrows in Fig. 3 indicate the directions of propagation of the lamellar structures. The behavior is similar to that reported by Hildebrand *et al.* [5] in surface chemical reaction systems, although the evolution equations are quite different.

B. Traveling hexagonal pattern

One of the characteristic features of the present model system (16) and (17) with Eqs. (19) and (20) is that not only lamellar patterns but also hexagonal structures can undergo coherent propagation by with appropriate values ψ_0 and ϕ_0.

Figure 4 shows one example for $\psi_0=-0.20$, $\phi_0=0.40$, where three snapshots of $\psi(\mathbf{r},t)$ are displayed in gray scale increasing from black to white at $t=50$ (a), 500 (b), and 5000 (c) for $\tau=1.6$ and $\gamma_2=0.1$. At the early stage, droplet-like domains move irregularly, accompanied by breakups and coalescence of domains [Figs. 4(a) and 4(b)] and finally form a regular hexagonal pattern traveling in one direction at a constant speed [Fig. 4(c)]. The propagation direction of the hexagons is indicated by white arrows in Fig. 4.

Another type of traveling hexagons appears in Fig. 5, where three snapshots of $\psi(\mathbf{r},t)$ at $t=50$ (a), 500 (b), and 5000 (c) are displayed for $\tau=2.0$ and $\gamma_2=0.06$ ($\psi_0=-0.33$, $\phi_0=0.50$). The transient behavior of this system is similar to that shown in Fig. 4. However, the propagation direction (white arrows in this figure) in the asymptotic state is perpendicular to that of the primary wave vectors.

Thus, it is found that there are at least two different types of traveling hexagons. Hereafter, we call the case shown in Fig. 4 type I and that in Fig. 5 type II.

Several ''phases'' of nonequilibrium states have been obtained by carrying out the simulations for various parameters. Figure 6 summarizes, in the parameter space (γ_2,τ), the various dynamic structures in two dimensions. The symbols indicate stationary lamellar structures (closed squares), traveling lamellar structures (open circles), traveling hexagonal structures of type I (crosses), traveling hexagonal structures of type II (pluses), and the uniform stable state (open square). For some parameters we could not distinguish between type I and type II hexagons within the present simulations. Such parameters are plotted with asterisks in Fig. 6.

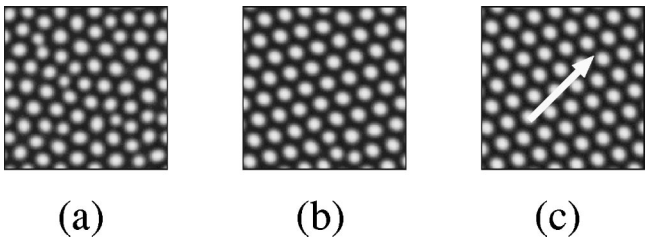

FIG. 5. Snapshots of $\psi(\mathbf{r},t)$ indicated in gray scale increasing from black to white at $t=50$ (a), 500 (b), and 5000 (c) for $\tau=2.0$ and $\gamma_2=0.06$. The white arrow indicates the direction of propagation of the hexagonal structure (type II).

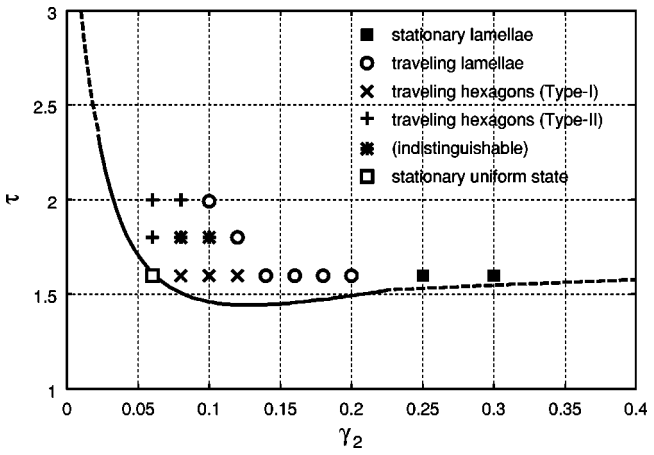

FIG. 6. Parameter dependence of the nonequilibrium states in (γ_2,τ) space. The symbols indicate stationary lamellar structures (closed squares), traveling lamellar structures (open circles), traveling hexagonal structures of type I (crosses), traveling hexagonal structures of type II (pluses), and the stationary uniform state (open square). The asterisks mean the states where we could not distinguish between type-I and type-II hexagons within the present simulations. The Hopf and Turing instability lines are also shown for convenience; they are the same as those in Fig. 1.

In this figure the Hopf and Turing instability lines are also shown for convenience; they are the same as those in Fig. 1.

It is noted here that the value of $\phi(\mathbf{r},t)$, which is the sum of the local concentrations of A and B molecules, becomes negative in some parameter regions. This shortcoming is due to the simplification of the free energy given by Eq. (12). However, we carried out the simulations avoiding this parameter region and believe that the results obtained would not be altered even if a more refined free energy were employed.

The amplitude of the traveling waves is plotted in Fig. 7 for both lamellar (open circles) and hexagonal (crosses) structures. It is evident that the bifurcation for lamellae is supercritical whereas that for hexagons is subcritical.

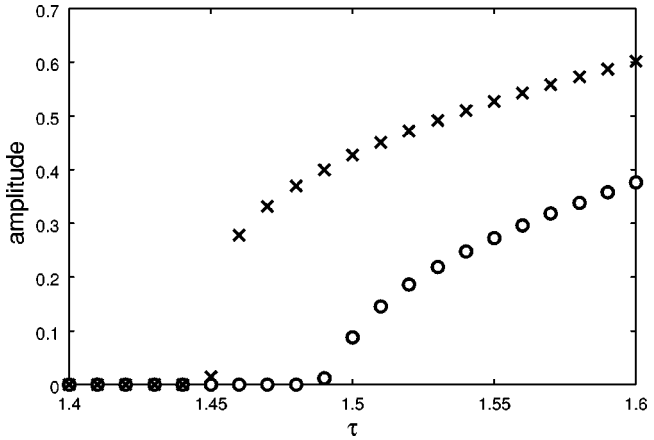

FIG. 7. Amplitudes of ψ in the traveling state for the lamellar (open circles) [$\gamma_1=0.3$, $\gamma_2=0.2$, and $\gamma_3=0.05$] and hexagonal (crosses) [$\gamma_1=0.3$, $\gamma_2=0.1$, and $\gamma_3=0.05$] structures as functions of the control parameter τ.

In order to verify that the emergence of traveling waves is quite general in the present model system, we carried out systematic simulations for a smaller value of τ, i.e., $\tau=0.2$. Setting the other parameters as $\gamma_1=0.005$ and $\gamma_3=0.0001$, the bifurcation line in Fig. 1 shifts downward and $\tau_c\approx 0.16$–0.17 depending on the reaction rate γ_2. We found that stable propagating lamellae appear for $\gamma_2=0.0012$, traveling hexagons of type I appear for $\gamma_2=0.0009$, and those of type II appear for $\gamma_2=0.0008$. These are the same tendencies as those shown in Fig. 6. When $\gamma_2=0.001$, we found an oscillation such that two kinds of lamellae perpendicular to each other are formed alternately. A similar pattern for a different set of parameters has also been obtained near the point where the Turing-type and Hopf-type bifurcation lines cross [23]. Although we carefully changed the parameter γ_2 step by step, the coexistence of motionless and propagating lamellae [21] was not observed in the present model system. Finally, we mention that the propagating waves are robust once they are formed. Any destabilization of the waves has not been realized. This will be confirmed theoretically for the lamellar pattern in the next section.

IV. THEORETICAL ANALYSIS OF TRAVELING LAMELLAE

The computer simulations given in the previous section show that the lamellar structure exhibits self-organized coherent propagation above the Hopf bifurcation threshold. It should be noted that a standing oscillation has never been observed in simulations. In order to understand this property, we derive the amplitude equation post-threshold and examine the stability of the oscillatory domains.

A. Amplitude equation

We study the time-evolution equations (16)–(20) in one dimension near the Hopf bifurcation point at the critical wave number q_c in the weakly nonlinear regime. The amplitude equation for Eqs. (16) and (17) near the Hopf instability line is derived by means of the usual reductive perturbation method [24,25], assuming that the bifurcation is supercritical, which is indeed the case as is shown in Fig. 7.

Near the bifurcation point, the most unstable mode $\mathbf{U}(x,t)$ is the relevant number of degrees of freedom of Eqs. (16) and (17), that is, $\mathbf{u}\sim\mathbf{u}_0+\mathbf{U}$, where $\mathbf{u}\equiv(\psi,\phi)^T$ and $\mathbf{u}_0\equiv(\psi_0,\phi_0)^T$. In terms of the eigenfunctions $\mathbf{U}_L$ and $\mathbf{U}_R$ defined below, the unstable mode $\mathbf{U}(x,t)$ is expressed as

$$\mathbf{U}(x,t)=W_L(x,t)\mathbf{U}_L+W_R(x,t)\mathbf{U}_R+\text{c.c.}, \tag{28}$$

where c.c. denotes the complex conjugate and $W_L(x,t)$ and $W_R(x,t)$ are the complex amplitudes of the plane wave solution propagating to the left and right, respectively. The wave number q_c and the frequency ω_c of the plane wave are determined by the eigenvalue problem

$$(\partial_t-\mathcal{L}_{q_c})\mathbf{U}_L=0, \tag{29}$$

where ∂_t denotes the partial differential operator with respect to t ($\mathbf{U}_R$ also satisfies the same equation). For the present problem, we choose

$$\mathbf{U}_L=\begin{pmatrix}1\\ \alpha\end{pmatrix}e^{iq_cx+i\omega_ct},\quad \mathbf{U}_R=\begin{pmatrix}1\\ \alpha\end{pmatrix}e^{-iq_cx+i\omega_ct} \tag{30}$$

with $\alpha\equiv(a_{22}+i\omega_c)/a_{12}$ and ω_c (>0) given by

$$\omega_c^2=\det\mathcal{L}_{q_c}=-a_{22}^2-a_{12}a_{21}. \tag{31}$$

By the standard procedure of perturbation [24,25], the final amplitude equations for W_L and W_R are given, respectively, by

$$\partial_tW_L=\mu W_L+b\partial_x^2W_L-g|W_L|^2W_L-h|W_R|^2W_L, \tag{32}$$

$$\partial_tW_R=\mu W_R+b\partial_x^2W_R-g|W_R|^2W_R-h|W_L|^2W_R, \tag{33}$$

where all the coefficients are complex and are given by

$$\mu\equiv\frac{\tilde{\tau}}{2}q_c^2\left(1+\frac{ia_{22}}{\omega_c}\right), \tag{34}$$

$$b\equiv 2D_1q_c^2\left(1+\frac{ia_{22}}{\omega_c}\right), \tag{35}$$

$$g\equiv\frac{3}{2}q_c^2\left(1+\frac{ia_{22}}{\omega_c}\right)\left[1+24\psi_0^2q_c^2\times\frac{a_{22}-2i\omega_c}{9(a_{11}+a_{22})(a_{22}-2i\omega_c)-3\omega_c^2}\right], \tag{36}$$

$$h\equiv 3q_c^2\left(1+\frac{ia_{22}}{\omega_c}\right)\left[1+24\psi_0^2q_c^2\frac{a_{22}}{9(a_{11}+a_{22})a_{22}+\omega_c^2}\right], \tag{37}$$

and $\tilde{\tau}\equiv\tau-\tau_c$ with the critical value τ_c of τ at which the bifurcation occurs. The constant g should not be confused with the function in Eq. (20). This type of amplitude equation was also obtained in Refs. [26,27]. Note that Eqs. (32) and (33) do not have terms proportional to ∂_xW_L or ∂_xW_R. This reflects the fact that in our model the group velocity is always zero, that is, $d\omega(q_c)/dq=0$, where $\omega(q)\equiv\sqrt{\det\mathcal{L}_q}$ near the bifurcation point. This comes from the particular choice of $D_2=0$ in Eq. (3). This will be discussed in Sec. VI.

B. Stability of the traveling wave

Here we examine the stability of the traveling wave solution of Eqs. (32) and (33). These equations have a set of solutions $W_L^{(0)}$ and $W_R^{(0)}$ as

$$W_L^{(0)}=0,\quad W_R^{(0)}=N_0e^{-iqx+i\Omega_0(q)t}, \tag{38}$$

where the real constants Ω_0 and N_0 are given by

$$N_0^2=\frac{1}{g_1}(\mu_1-b_1q^2), \tag{39}$$

$$\Omega_0=\mu_2-b_2q^2-\frac{g_2}{g_1}(\mu_1-b_1q^2), \tag{40}$$

and $\mu=\mu_1+i\mu_2$, $b=b_1+ib_2$ with real numbers μ_1, μ_2, b_1, and b_2. A similar notation has also been utilized for g and h.

In order to study the stability of the solution (38), let us introduce deviations ξ and η as

$$W_L=W_L^{(0)}+\xi, \tag{41}$$

$$W_R=W_R^{(0)}+\eta. \tag{42}$$

Substituting Eqs. (41) and (42) into Eqs. (32) and (33) yields up to the first order of the deviations

$$\partial_t\xi=\mu\xi+b\partial_x^2\xi-hN_0^2\xi, \tag{43}$$

$$\partial_t\eta=\mu\eta+b\partial_x^2\eta-(W_R^{(0)})^2\bar{\eta}-2gN_0^2\eta, \tag{44}$$

where $\bar{\eta}$ is the complex conjugate to η. Setting $\xi\propto\exp(iqx+\lambda t)$, we obtain

$$\lambda=\mu-bq^2-hN_0^2. \tag{45}$$

The growth rate of the deviation ξ is given by

$$\mathrm{Re}\,\lambda=(\mu_1-b_1q^2)\left(1-\frac{h_1}{g_1}\right), \tag{46}$$

where we have used Eq. (39). Since $(\mu_1-b_1q^2)/g_1=N_0^2>0$, we need the stability condition for the traveling wave [26,27]

$$h_1>g_1. \tag{47}$$

Next, we investigate the stability of the standing wave solution given by

$$W_L^{(0)}=N_0e^{iqx+i\Omega_0t},\quad W_R^{(0)}=N_0e^{-iqx+i\Omega_0t}, \tag{48}$$

where Ω_0 and N_0 satisfy the following relation:

$$i\Omega_0=\mu-bq^2-gN_0^2-hN_0^2. \tag{49}$$

We introduce small deviations of the amplitudes $\xi(x,t)$, $\eta(x,t)$ and the phases $\varphi(x,t),\theta(x,t)$ as

$$W_L=N_0(1+\xi)e^{iqx+i\Omega_0t+i\varphi}, \tag{50}$$

$$W_R=N_0(1+\eta)e^{-iqx+i\Omega_0t+i\theta}. \tag{51}$$

From Eqs. (32), (33), (50), and (51) we obtain the time-evolution equations for the deviations. The deviations of the amplitudes obey up to the first order

$$\partial_t \xi = -2g_1 N_0^2 \xi - 2h_1 N_0^2 \eta + b_1 \partial_x^2 \xi - 2qb_2 \partial_x \xi - 2qb_1 \partial_x \varphi - b_2 \partial_x^2 \varphi, \tag{52}$$

$$\partial_t \eta = -2g_1 N_0^2 \eta - 2h_1 N_0^2 \xi + b_1 \partial_x^2 \eta + 2qb_2 \partial_x \eta + 2qb_1 \partial_x \theta - b_2 \partial_x^2 \theta, \tag{53}$$

where we have used Eq. (49). In the long wavelength limit, we may retain only the first two terms of Eqs. (52) and (53). In this case, the eigenvalues of the time-evolution matrix are

$$\lambda = -2N_0^2 (g_1 \pm h_1). \tag{54}$$

Since g_1 is positive when the bifurcation is supercritical, we have the stability condition of the standing wave [26,27]:

$$-g_1 < h_1 < g_1. \tag{55}$$

According to numerical calculations based on Eqs. (36) and (37), we did not find parameters for which the standing wave is stable as long as $g_1 > 0$. This agrees with the fact that we never found a standing wave in the simulations of Eqs. (16)–(20).

C. Phase dynamics for traveling waves

Now we discuss the phase dynamics for the traveling wave solution. We write a solution of Eqs. (32) and (33) with the deviations $\xi(x,t)$ and $\varphi(x,t)$ as

$$W_L = 0, \quad W_R = N_0 (1+\xi) e^{-iqx + i\Omega_0 t + i\varphi}. \tag{56}$$

The zeroth order solution was obtained in Eqs. (38). The first order equations are given by

$$\partial_t \xi = -2g_1 N_0^2 \xi + b_1 \partial_x^2 \xi + 2qb_2 \partial_x \xi + 2qb_1 \partial_x \varphi - b_2 \partial_x^2 \varphi, \tag{57}$$

$$\partial_t \varphi = -2qb_1 \partial_x \varphi + b_1 \partial_x^2 \varphi + b_2 \partial_x^2 \xi + qb_2 \partial_x \varphi - 2g_2 N_0^2 \xi. \tag{58}$$

Since the amplitude deviation decays rapidly compared with the phase deviation in the long wavelength modulation, we may eliminate ξ adiabatically by putting $\partial_t \xi = 0$ in Eq. (57), so that we have

$$\xi = \frac{1}{2g_1 N_0^2} (2qb_1 \partial \varphi - b_2 \partial_x^2 \varphi + 2qb_2 \partial_x \xi + b_1 \partial_x^2 \xi). \tag{59}$$

Applying Eq. (59) iteratively, we obtain the following expression for ξ as a gradient expansion of φ [26,27]:

$$\xi = \frac{qb_1}{g_1 N_0^2} \partial_x \varphi + \frac{b_2}{2g_1 N_0^2} \left(-1 + \frac{2q^2 b_1}{g_1 N_0^2} \right) \partial_x^2 \varphi + \cdots. \tag{60}$$

Substituting Eq. (60) into Eq. (58), we obtain up to the second order derivatives of ϕ

$$\partial_t \varphi = C \partial_x \varphi + D \partial_x^2 \varphi, \tag{61}$$

where

$$C \equiv 2q \left(b_2 - \frac{g_2}{g_1} b_1 \right), \tag{62}$$

$$D \equiv \left(b_1 + \frac{g_2}{g_1} b_2 \right) \left(1 - \frac{2q^2 b_1}{g_1 N_0^2} \right). \tag{63}$$

Here we consider the case where the factor $b_1 + g_2 b_2 / g_1$ in Eq. (63) is positive, so that the traveling wave solution is stable for $|q| \to 0$. In this case, the coefficient D becomes negative for large values of $|q|$, which causes an Ekhaus-type instability. Since $1 - 2q^2 b_1 / (g_1 N_0^2) = (\mu_1 - 3q^2 b_1) / (g_1 N_0^2)$, this instability occurs when

$$q^2 > \frac{\mu_1}{3b_1}. \tag{64}$$

Note from Eq. (39) that the condition $q^2 < \mu_1 / b_1$ is required for the traveling wave solution to exist.

We can obtain amplitude equations for traveling lamellar structures which are similar to the equation for the one-dimensional case. The complex amplitudes $W_L(\mathbf{r},t)$ and $W_R(\mathbf{r},t)$ of waves propagating to the left and right in the x direction obey the following equations, corresponding to Eqs. (32) and (33):

$$\partial_t W_L = \mu W_L + b \left(\partial_x - \frac{i}{2q_c} \partial_y^2 \right)^2 W_L - g |W_L|^2 W_L - h |W_R|^2 W_L, \tag{65}$$

$$\partial_t W_R = \mu W_R + b \left(\partial_x - \frac{i}{2q_c} \partial_y^2 \right)^2 W_R - g |W_R|^2 W_R - h |W_L|^2 W_R, \tag{66}$$

where the coefficients μ, b, g, and h are defined in Eqs. (34)–(37).

We can also develop the phase dynamics in two dimensions from the above amplitude equation. We write a traveling wave solution of Eqs. (65) and (66) propagating in the x direction as

$$W_L = 0, \quad W_R = N_0 [1 + \xi(\mathbf{r},t)] e^{-iqx + i\Omega_0 t + i\varphi(\mathbf{r},t)}, \tag{67}$$

where $\xi(\mathbf{r},t)$ and $\varphi(\mathbf{r},t)$ are the small deviations associated with the amplitude and phase, respectively. Repeating the same procedure shown above, we obtain the phase equation corresponding to Eq. (61) as

$$\partial_t \varphi = C \partial_x \varphi + D \partial_x^2 \varphi - \frac{q}{q_c} \left(b_1 + \frac{g_2}{g_1} b_2 \right) \partial_y^2 \varphi, \tag{68}$$

where C and D are given by Eqs. (62) and (63), respectively. Equation (68) implies that when $q > 0$ the phase deviation in the y direction is destabilized. This corresponds to a zigzag-type instability.

In the numerical simulations shown in Sec. III we never found either Ekhaus- or zigzag-type instabilities. We should say that the traveling wave solution is quite stable in our model system.

V. THEORETICAL ANALYSIS OF TRAVELING HEXAGONS

In two-dimensional systems, not only a lamellar structure but also a hexagonal structure is allowed to exist as a spatially periodic structure. As was shown in the previous section, the hexagonal structure also undergoes coherent propagation above the Hopf instability line.

We do not carry out a systematic derivation of the amplitude equations for the traveling hexagons mainly because the bifurcation is subcritical and hence evaluation of each coefficient of the amplitude equation is more involved. Here we employ a simple mode expansion focusing on the two types of the traveling pattern obtained in the simulations.

We seek a solution of Eqs. (16) and (17) in the form $\psi(\mathbf{r},t)=\hat{\psi}(\mathbf{r}-\mathbf{V}t)$, $\phi(\mathbf{r},t)=\hat{\phi}(\mathbf{r}-\mathbf{V}t)$, with a traveling velocity $\mathbf{V}$. Here we make the approximation that the functions $\hat{\psi}(\mathbf{r})$ and $\hat{\phi}(\mathbf{r})$ are represented in terms of the lowest Fourier modes as

$$\hat{\psi}(\mathbf{r})=\sum_{k=-3}^{3}\hat{\psi}_{\mathbf{q}_k}e^{i\mathbf{q}_k\cdot\mathbf{r}},\quad \hat{\phi}(\mathbf{r})=\sum_{k=-3}^{3}\hat{\phi}_{\mathbf{q}_k}e^{i\mathbf{q}_k\cdot\mathbf{r}},\quad (69)$$

where $\mathbf{q}_k\equiv(q_c\cos(2\pi/3)k, q_c\sin(2\pi/3)k)$ $(k=\pm1,\pm2,\pm3)$ and $\mathbf{q}_0\equiv\mathbf{0}$. Note that $\hat{\psi}_{\mathbf{q}_0}=\psi_0$ and $\hat{\phi}_{\mathbf{q}_0}=\phi_0$. We have verified numerically that the actual spatial profile does not deviate substantially from Eq. (69) near the Hopf bifurcation line although it is subcritical.

From Eqs. (16), (17), and (69), we obtain a set of equations for $\hat{\psi}_{\mathbf{q}_k}$, $\hat{\phi}_{\mathbf{q}_k}$, and $\mathbf{V}$. Eliminating $\hat{\phi}_{\mathbf{q}_k}$ and introducing the real amplitude A_k and the phase θ_k as $\hat{\psi}_{\mathbf{q}_k}=A_k\exp(i\theta_k)$, we finally obtain

$$\Omega(\omega_k)A_k=\mu A_k-3q_c^2[2\psi_0A_lA_me^{-i\varphi}+A_k^3+2(A_l^2+A_m^2)A_k] \quad (70)$$

for $k=1,2,3$ $[l,m=k+1,k+2 \pmod 3]$ with

$$\Omega(\omega)\equiv\frac{\omega^2-\omega_c^2}{\omega^2+a_{22}^2}(a_{22}-i\omega), \quad (71)$$

where $\varphi\equiv\theta_1+\theta_2+\theta_3$, $\mu\equiv-q_c^2(Dq_c^2-\tilde{\tau})-(\gamma_1+\gamma_2+\gamma_3)$, $\omega_k\equiv\mathbf{q}_k\cdot\mathbf{V}$, and $\omega_c\equiv\mathrm{Im}\ \lambda(q_c)$ is the critical frequency at the Hopf bifurcation point. Note that two of the three phase variables θ_k are arbitrary and only the sum φ is determined by the above equations. Therefore, Eqs. (70) and (71) under the condition $\omega_1+\omega_2+\omega_3=0$ determine A_k, φ, and $\mathbf{V}$.

When $A_k\neq0$, the imaginary part of Eq. (70) gives

$$-\omega_k\frac{\omega_k^2-\omega_c^2}{\omega_k^2+a_{22}}=6q_c^2\psi_0\frac{A_lA_m}{A_k}\sin\varphi. \quad (72)$$

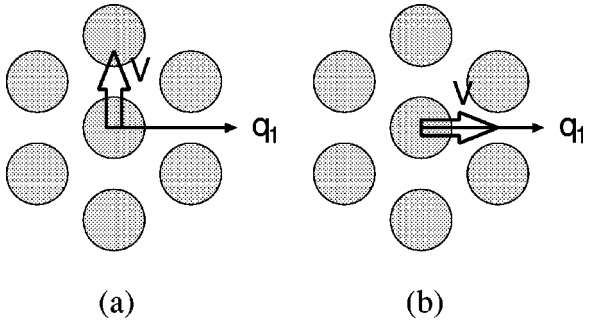

FIG. 8. Schematic picture of the directions of traveling velocity $\mathbf{V}$ and wave vector $\mathbf{q}_1$ for traveling hexagonal domains of type I (a) and type II (b). Thick and thin arrows indicate the directions of $\mathbf{V}$ and $\mathbf{q}_1$, respectively, and the hatched regions represent ψ-rich domains.

In the special case that $\sin\varphi=0$, Eq. (72) has the solutions $\omega_k=0$ and $\pm\omega_c$. If we choose $\omega_1=0$, $\omega_2=\omega_c$, and $\omega_3=-\omega_c$, then the traveling velocity $\mathbf{V}$ is perpendicular to $\mathbf{q}_1$ [see Fig. 8(a)]. This is the type-I solution. On the other hand, the type-II solution of Eq. (70) is represented as $\omega_1=-2\omega_2$ and $\omega_2=\omega_3$, which the condition $\omega_1+\omega_2+\omega_3=0$. In this case, $\mathbf{V}$ is indeed parallel to $\mathbf{q}_1$ as shown in Fig. 8(b).

VI. CONCLUDING REMARKS

In this paper, we constructed a model equation for phase separation of chemically reactive ternary mixtures. In this model the thermodynamic destabilization induces a Turing- or Hopf-type instability at a finite wave number, depending on the parameters in the reaction terms. The phase diagram for the nonequilibrium states was obtained numerically. The traveling waves appear as a Hopf bifurcation at a finite wavenumber. In two-dimensional simulations we obtained a traveling lamellar structure and two types (type I and type II) of traveling hexagonal structures.

We derived the amplitude equations for the supercritical Hopf bifurcation at a finite wave number from the model equations and investigated the stability of traveling waves and standing oscillations in one-dimensional systems. The traveling wave is found to be stable in some parameter regions. However, we have never found, at least numerically, any region in which a standing oscillation is stable. The mathematical structure of the two types of traveling hexagons has been clarified by the amplitude equations derived by the single mode approximation in two dimensions. However, in order to make a full comparison with the phase diagram shown in Fig. 6, obtained numerically, one needs a stability analysis of the traveling hexagonal patterns, which is more involved mathematically and is beyond the scope of the present study.

In the present set of model equations (16) and (17), we omitted the diffusion of ϕ. As a consequence, the group velocity of the traveling waves turns out to be identically zero, as mentioned in Sec. IV A. However, it was shown in Ref. [26] that the stability conditions (47) and (55) for traveling lamellar domains are unaltered when the group velocity is finite. Furthermore, we carried out additional simulations

by adding the diffusion term $K\nabla^2\phi$ on the right-hand side of Eq. (17). Although we do not exclude the possibility that other spatiotemporal patterns might appear when $K\neq 0$, we obtained essentially the same traveling waves, e.g., for the fixed values of $K=0.05$, $D_1=1$, $\gamma_1=0.3$, $\gamma_3=0.01$, and several values of γ_2 and τ.

There is a simple explanation as to why one needs three components of chemical species for coherently propagating domains. Suppose that the species are arrayed in one-dimensional space as A,B,C,A. After one cycle of chemical reaction, this order becomes B,C,A,B. This means that the domains are moving to the left. It is clear from this argument that the relative phase difference of the chemical reaction determines the propagation direction and that a standing oscillation is quite unlikely in the present system.

What we have shown in this paper is that phase transitions in nonequilibrium conditions produce a rich variety of self-organized domain dynamics, which never occur in thermal equilibrium where the ordered state is motionless and is simply uniform or at most modulated in space. Although we do not know, at present, any concrete materials for phase-separating reactive ternary mixtures, we hope that the present study will trigger further experiments for mesoscopic domain dynamics far from equilibrium.

Thermal fluctuations have been believed to be unimportant for pattern formation far from equilibrium as far as macroscopic patterns such as Rayleigh-Bénard convection and Belousov-Zhabotinski reaction are concerned. (See, however, the recent experiments [28] for electroconvection of liquid crystals.) In contrast, when the domain structure is of microscopic scale as in the present model system, thermal fluctuations cannot be ignored near the bifurcation points out of equilibrium and might qualitatively alter the properties of the transition. Concentration fluctuations around the deterministic motion may also exhibit some characteristic features inherent to nonequilibrium systems. We hope to return to these fundamental problems elsewhere in the future.

ACKNOWLEDGMENTS

We would like to thank Professor A. S. Mikhailov for valuable discussions. This work was supported by a Grant-in-Aid for Scientific Research from the Ministry of Education, Science, Sports and Culture of Japan.

[1] M. C. Cross and P. C. Hohenberg, Rev. Mod. Phys. **65**, 851 (1993).
[2] A. Joets and R. Ribotta, Phys. Rev. Lett. **60**, 2164 (1988).
[3] R. Imbihl and G. Ertl, Chem. Rev. (Washington, D.C.) **95**, 697 (1995).
[4] A. von Oertzen, H. H. Rotermund, A. S. Mikhailov, and G. Ertl, J. Phys. Chem. B **104**, 3155 (2000).
[5] M. Hildebrand, A. S. Mikhailov, and G. Ertl, Phys. Rev. Lett. **81**, 2602 (1998).
[6] A. S. Mikhailov, M. Hildebrand, and G. Ertl, in *Coherent Structures in Classical Systems*, edited by M. Rubi *et al.* (Springer, New York, 2001), and references cited therein.
[7] Y. Tabe and H. Yokoyama, Langmuir **11**, 4609 (1995).
[8] R. Reigada, F. Sagués, and A. S. Mikhailov, Phys. Rev. Lett. **89**, 038301 (2002).
[9] B. A. Huberman, J. Chem. Phys. **65**, 2013 (1976).
[10] S. C. Glotzer, E. A. Di Marzio, and M. Muthukumar, Phys. Rev. Lett. **74**, 2034 (1995).
[11] J. Verdasca, P. Borckmans, and G. Dewel, Phys. Rev. E **52**, R4616 (1995).
[12] M. Motoyama and T. Ohta, J. Phys. Soc. Jpn. **66**, 2715 (1997).
[13] Q. Tran-Cong and A. Harada, Phys. Rev. Lett. **76**, 1162 (1996).
[14] T. Ohta and K. Kawasaki, Macromolecules **19**, 2621 (1986).
[15] M. Bahiana and Y. Oono, Phys. Rev. A **41**, 6763 (1990).
[16] J. D. Gunton, M. San Miguel, and P. S. Sahni, in *Phase Transitions and Critical Phenomena*, edited by C. Domb and J. L. Lebowitz (Academic, New York, 1983), Vol. 8.
[17] A. J. Bray, Adv. Phys. **43**, 357 (1994).
[18] I. Daumont, K. Kassner, C. Misbah, and A. Valance, Phys. Rev. E **55**, 6902 (1997).
[19] C. B. Price, Phys. Rev. E **55**, 6698 (1997).
[20] T. Okuzono and T. Ohta, Phys. Rev. E **64**, 045201 (2001).
[21] E. M. Nicola, M. Or-Guil, W. Wolf, and M. Bär, Phys. Rev. E **65**, 055101 (2002).
[22] S. A. Safran, *Statistical Thermodynamics of Surfaces, Interfaces, and Membranes* (Addison-Wesley, Tokyo, 1994).
[23] S. Sugiura, T. Okuzono, and T. Ohta, Phys. Rev. E **66**, 066216 (2002).
[24] Y. Kuramoto, *Chemical Oscillations, Waves and Turbulence* (Springer-Verlag, Berlin, 1984).
[25] D. Walgraef, *Spatio-Temporal Pattern Formation* (Springer-Verlag, New York, 1997).
[26] P. Coullet, S. Fauve, and E. Tirapegui, J. Phys. (France) Lett. **46**, L-787 (1985).
[27] T. Ohta and K. Kawasaki, Physica D **27**, 21 (1987).
[28] M. A. Scherer and G. Ahlers, Phys. Rev. E **65**, 051101 (2002).